ACS APPLIED MATERIALS & INTERFACES

Research Article

www.acsami.org

A Ratiometric Fluorescent Probe Based on ESIPT and AIE Processes for Alkaline Phosphatase Activity Assay and Visualization in Living Cells

Zhegang Song,[†,‡,∥] Ryan T. K. Kwok,[†,‡,∥] Engui Zhao,[†,‡] Zikai He,[†,‡] Yuning Hong,[†,‡] Jacky W. Y. Lam,[†,‡] Bin Liu,*[,§] and Ben Zhong Tang*[,†,‡,⊥]

[†]HKUST Shenzhen Research Institute, No. 9 Yuexing First RD, South Area, Hi-Tech Park, Nanshan, Shenzhen, China 518057

[‡]Department of Chemistry, Institute for Advanced Study, Division of Biomedical Engineering, Division of Life Science, State Key Laboratory of Molecular Neuroscience, and Institute of Molecular Functional Materials, The Hong Kong University of Science and Technology, Clear Water Bay, Kowloon, Hong Kong, China

[§]Department of Chemical and Biomolecular Engineering, National University of Singapore, 4 Engineering Drive 4, Singapore 117585

[⊥]Guangdong Innovative Research Team, SCUT-HKUST Joint Research Laboratory, State Key Laboratory of Luminescent Materials and Devices, South China University of Technology, Guangzhou, China 510640

Supporting Information

ABSTRACT: Alkaline phosphatase (ALP) activity is regarded as an important biomarker in medical diagnosis. A ratiometric fluorescent probe is developed based on a phosphorylated chalcone derivative for ALP activity assay and visualization in living cells. The probe is soluble in water and emits greenish-yellow in aqueous buffers. In the presence of ALP, the emission of probe changes to deep red gradually with ratiometric fluorescent response due to formation and aggregation of enzymatic product, whose fluorescence involves both excited-state intramolecular proton transfer and aggregation-induced emission processes. The linear ratiometric fluorescent response enables *in vitro* quantification of ALP activity in a range of 0−150 mU/mL with a detection limit of 0.15 mU/mL. The probe also shows excellent biocompatibility, which enables it to apply in ALP mapping in living cells.

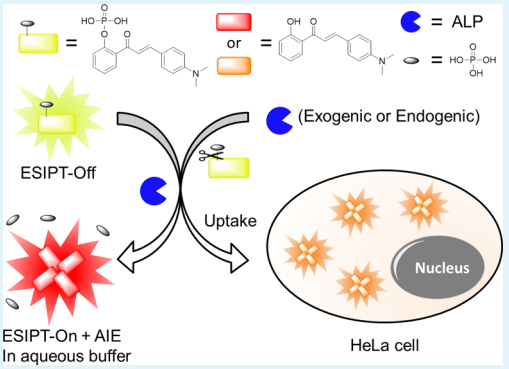

KEYWORDS: *ratiometric fluorescent probe, aggregation-induced emission, alkaline phosphatase, bioprobe, ESIPT*

1. INTRODUCTION

Disease diagnosis attracts much attention from researchers, clinical doctors, and medical companies since early detection of severe diseases (e.g., cancers and AIDS) is of critical importance to prevent disease progression and increase clinical cure rate.[1,2] Thank to the enthusiastic efforts of the scientists, a variety of bioprobes for specific diseases with high sensitivity and selectivity have been developed.[3−6] Alkaline phosphatase (ALP) is a hydrolase that catalyzes the dephosphorylation process of various substrates including nucleic acids, proteins, and carbohydrates, and its activity is often regarded as an important biomarker in medical diagnosis.[7,8] The normal level of ALP activity in human serum is in a range of 40−150 mU/mL. Abnormal levels of ALP activity in serum may reflect several diseases, such as hepatitis, prostatic cancer, osteoporosis, and bone tumor.[9−11] In addition, as a series of secreted proteins, ALP activity in extracelluar fluid also indicates the viability of local cells. Thus, real-time monitoring of ALP-expressing cell viability is necessary to distinguish normal and abnormal behavior of cells (e.g., hyperproliferation).[12,13]

Fluorescent probes, with their intrinsic advantages of low background noise and high sensitivity, are excellent candidates not only in the area of bioassay *in vitro*, but also in the visualization of targeting analytes in living cells.[14−18] Many fluorescent probes have been developed for monitoring ALP activity by different mechanisms, including host−guest interaction, assembly of nanoparticles, change of solubility, and self-assembling of heteroaggregation.[19−23] For example, Ji et al. realized a turn-off ALP assay by the adoption of β-cyclodextrin-modified quantum dots as fluorescent reporter and *p*-nitrophenyl phosphate as the substrate. In the presence of ALP, the *p*-nitrophenyl phosphate is catalytically converted to *p*-nitrophenol, which quenches the fluorescence of quantum dots based on host−guest interaction and energy transfer.[19] Yu and co-workers used pyrophosphate (PPi) and Cu^{2+} complex to hamper the formation of fluorescent copper nanoparticles (CuNPs), and the ALP activity is assayed through disassembling the complex, resulting in the formation of fluorescent CuNPs.[20] These probes, however, have some limitations such as low sensitivity, laborious synthetic procedures, and

Received: August 4, 2014
Accepted: September 11, 2014
Published: September 11, 2014

complicated sensing mechanisms as well as short emission wavelength.

Fluorogens with aggregation-induced emission (AIE) characteristics have recently emerged as a novel class of fluorescent materials with increasing applications in biosensing and imaging.[24−28] Unlike conventional systems, AIE fluorogens are nonemissive in solution but emit strongly in aggregated or solid states. Taking advantage of this unique property, a wide variety of AIE bioprobes have been reported in sensing different biomolecules with high sensitivity such as DNA, proteins, and sugars.[29,30] Recently, two AIE probes for ALP activity assay have been developed by Zhang and Liu et al., respectively, with high sensitivity and excellent selectivity.[31,32] However, these AIE probes emit blue or green color, which may be strongly influenced by the autofluorescence from living cells. Therefore, it is more desirable to design a fluorescent probe with red emission for ALP activity assay.

Excited-state intramolecular proton transfer (ESIPT) is a photochemical process occurring in the excited singlet state of a molecule with intramolecular hydrogen bond.[33] This process has been studied intensively in recent years because ESIPT usually alters the conjugation system of a fluorophore, thus inducing redder emission.[34−37] 2′-Hydroxychalcone (HC) and its derivatives were reported as a new class of fluorophores with ESIPT process.[38] The HC molecules undergo the ESIPT process through enol form to keto form and generate a well-conjugated structure with alternating single and double bonds (Scheme 1).

Scheme 1. ESIPT process of HCA

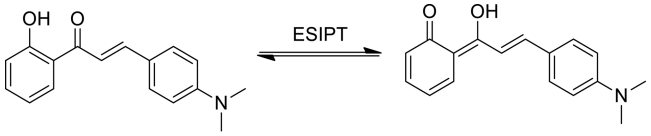

HCA (Normal form) HCA* (Keto form)

In this work, we report a ratiometric fluorescent probe (HCAP) with AIE attribute for ALP activity assay and visualization of ALP in living cells. The probe is water-soluble and emits greenish-yellow in aqueous buffers. In the presence of ALP, the phosphate group on HCAP is cleaved, resulting in formation of insoluble enzymatic product (HCA), which emits red fluorescence (Scheme 2). Since the yellow emission from HCAP decreases and the red emission from HCA increases upon ALP activity, a ratiometric fluorescent probe is developed. Meanwhile, the excellent biocompatibility of HCAP prompts us to utilize it to map the endogenic ALP in living cells.

Scheme 2. Schematic illustration of HCAP for ALP activity assay in solution and in living cells

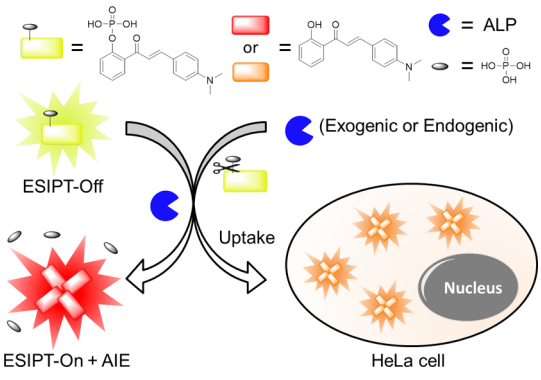

2. RESULTS AND DISCUSSION

2.1. Syntheses of HCA and HCAP. The synthetic route to HCA and HCAP is depicted in Scheme 3. HCA is synthesized with 2′-hydroxyacetophenone and 4-dimethylaminobenzaldehyde through Claisen−Schmidt condensation reaction under mild basic conditions with a yield of 22%.[38] HCA is purified through recrystallization to obtain red crystalline products. HCAPE was then synthesized through phosphorylation of HCA with diethyl chlorophosphate in the presence of sodium hydride. HCAPE was subsequently deprotected by iodotrimethylsilane to furnish HCAP. All compounds were purified and characterized by standard spectroscopic techniques including NMR and HRMS, from which satisfactory analysis data corresponding to their expected chemical structures were obtained (Supporting Information, Figures S1−S11).

2.2. Optical Property of HCA and HCAP. The optical property of HCA and HCAP was first investigated. HCA is a hydrophobic fluorophore and can readily dissolve in tetrahydrofuran (THF), while HCAP is a hydrophilic molecule and dissolves well in aqueous solution. As shown in Supporting Information, Figure S12, the absorption spectra of HCA in THF solution and HCAP in water exhibit absorption maximums at 430 and 416 nm, respectively. The blue-shifted absorption of HCAP is associated with steric repulsion of the bulky phosphate group. Such repulsion causes the benzoyl group on HCAP to be twisted. Thus, the π-conjugated system in HCAP is weakened, resulting in blue-shifted absorption. HCAP in aqueous solutions emits greenish-yellow fluorescence, which is originated from *N*,*N*-dimethylaniline and vinyl ketone moiety. Interestingly, HCA is nonemissive when dissolved in good solvents such as THF and dichloromethane (DCM), but its crystals show very strong red fluorescence (Φ_F = 18.5%) under UV excitation with 365 nm light (Supporting Information, Figure S12B). Such emission property of HCA may present the AIE signature. To further examine whether HCA is an AIE-active molecule, its photoluminescence (PL) property is investigated using THF and water solvent mixtures. As shown in Figure 1, HCA is nonemissive in pure THF. With increasing the water content in THF/water mixtures from 0 to 80%, the fluorescence intensity increases gradually, and the emission wavelength is red-shifted. Further addition of water into the mixture leads to a sharp and dramatic enhancement of PL intensity, and the emission maximum peak is shifted to 640 nm. At 90 vol % water content, the red fluorescence intensity is nearly 60-fold higher than that in the pure THF solution. Clearly, HCA is AIE-active. Different from typical AIE fluorogens like tetraphenylethene (TPE), whose fluorescence is induced to emit intensively only in aggregated state, HCA displays rather different emission properties in its solution and aggregated states. Besides that, the restriction of intramolecular rotation (RIR) theory for the typical AIE system is not capable of explaining such emission property of HCA.

To understand the origin of the AIE property of HCA, the single-crystal structure of HCA is disclosed by X-ray diffraction (Figure 2). From the crystal structure, the hydrogen-bonding geometry, with O(1)H···O(2) = 1.75 Å, reveals that there exists strong intramolecular hydrogen bonding, which facilitates the ESIPT process of HCA (Scheme 1).[39] Meanwhile, the crystal packing of HCA is mainly edge-to-face and head-to-head, in

Scheme 3. Synthetic Route to HCA and HCAP

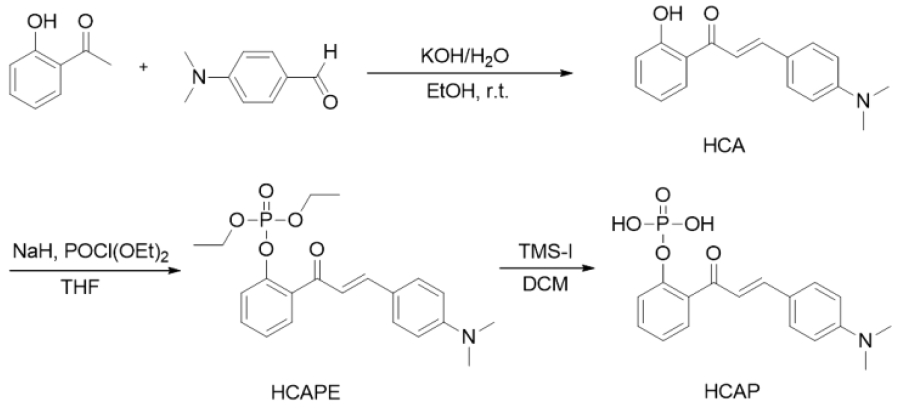

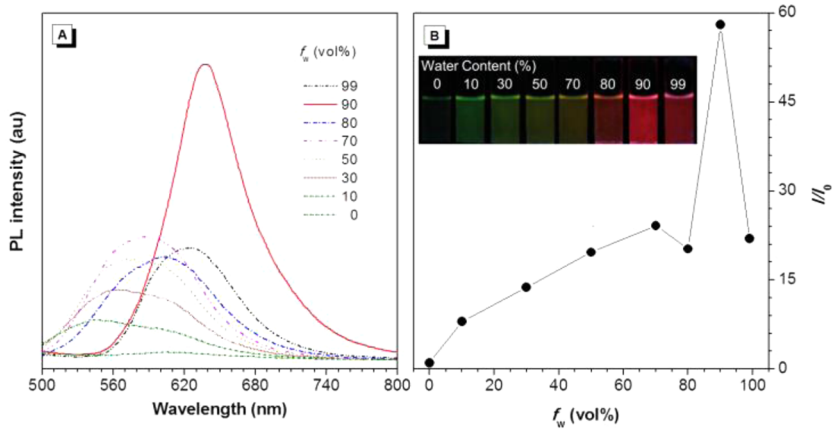

Figure 1. (A) PL spectra of HCA in THF/water mixtures with different water fractions (f_w). (B) Plot of relative peak intensity (I/I_0) vs f_w. Concentration: 20 μM; excitation wavelength: 430 nm. (inset) Photographs of HCA in THF/water mixtures with different water fractions taken under hand-held UV lamp with 365 nm illumination.

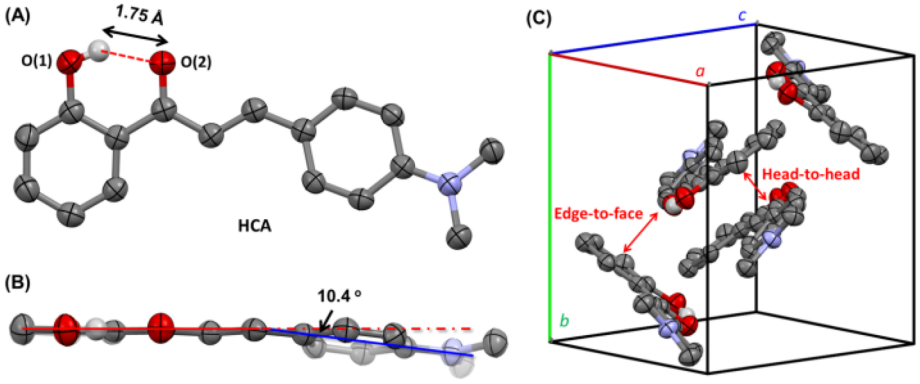

Figure 2. (A) ORTEP drawing of single-crystal structure of HCA with 50% probability ellipsoids and hydrogen bond geometry. (B) Side view of crystal structure of HCA. (C) A unit cell of the crystal structure.

which the $\pi-\pi$ interaction between the molecules is avoided. In pure THF solution, the HCA molecules are excited under UV illumination and ESIPT occurs, which generates various transition states or resonance structures, as well as isomerization if the molecular conformation is not fixed. Such processes serve as a relaxation channel for the excited state to decay.[39,40] When a small amount of water is added into the THF solution, the intramolecular hydrogen bonding is impaired, and the ESIPT process is inhibited. Thus, the mixture starts to emit a greenish-yellow emission like that of HCAP, and the emission intensity increases along with water fraction (f_w) from 10 to 80%. However, when more water is added, HCA is induced to form tiny crystals due to its poor water solubility. In the crystallizing state, the molecular conformation of HCA is fixed, and the water molecule is isolated from the HCA molecule. As a result, the intramolecular hydrogen bonding in HCA is reformed, and the ESIPT process brings the keto form of HCA to emit red fluorescence intensively.

2.3. Design and Sensing Principle. HCA shows excellent optical properties including absorption band in visible region and red emission in crystalline state, rendering it a superior

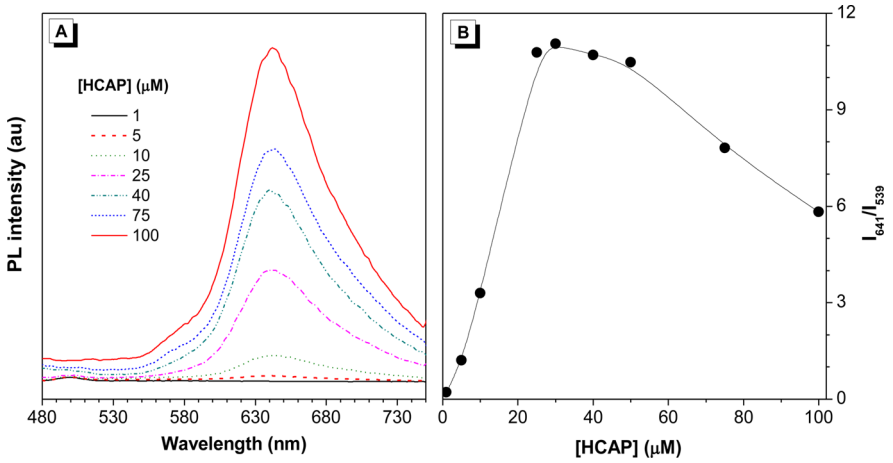

Figure 3. (A) PL spectra of HCAP in different concentrations after incubation with 100 mU/mL of ALP. (B) Plot of ratiometric fluorescence intensity (I_{641}/I_{539}) versus the concentration of HCAP; incubation time: 45 min; excitation wavelength: 430 nm.

candidate for fluorescent probes. Inspired by the importance of ALP activity assay and typical design strategy of ALP probes, we have modified HCA with a phosphate group, which serves as the recognition site of ALP. The sensing mechanism is illustrated in Scheme 2. HCAP is highly water-soluble and emits greenish-yellow in buffer solutions. In the presence of ALP, the phosphate group on HCAP will be cleaved, and HCA is reformed after protonation. Meanwhile, HCA easily forms crystals in aqueous media due to its poor water solubility and formation of intramolecular hydrogen bond. The crystallization of HCA will activate the AIE and ESIPT processes. As a result, the greenish-yellow fluorescence from HCAP will be diminished, while the red fluorescence from HCA crystals will be turned on during ALP-catalyzed process. Thus, the ratiometric fluorescence responding to ALP activity can be realized with the emission colors changing from greenish-yellow to red. Furthermore, ALP is widely distributed in cytosols, intercellular fluids, and serums of mammals. HCAP will be converted to HCA with the catalytic function of endogenic ALP secreted by cancer cells. Therefore, HCAP is also expected to act as a fluorescent probe for ALP detection in situ and visualization of ALP at cellular level.

2.4. Optimization of Fluorescent Sensing of ALP. To construct a sensitive fluorescent probe, the sensing conditions need to be optimized. Since HCA is pH-sensitive, the effect of pH on the emission intensity of HCA is evaluated. From the PL spectra shown in Figure 1, HCA shows the highest emission when the water content is 90%. Thus, in the optimization experiments, the buffer solutions with pH ranging from 2 to 12 were used to mix with THF at a ratio of 90:10 v/v. From the result depicted in Supporting Information, Figure S13, the result shows that the HCA emits intensely in a wide pH range (3−11); however, the emission is much weaker in both strong acidic or basic conditions. This is because in strong acidic conditions, the dimethylamino group is protonated, and the D−A system of HCA is destroyed. While in strong basic conditions, the hydroxyl group of HCA is deprotonated; therefore, the ESIPT process is lost in phenolate form. Meanwhile, the effect of pH on the emission intensity of HCAP was also examined (Supporting Information, Figure S14). The result shows the unperturbed optical property of HCAP in aqueous media when pH > 7. As the optimum pH for ALP is 9.2,[41] while HCA has a good work preferment in this pH value, we chose Tris-HCl buffer solution with pH 9.2 in further experiments.

For ratiometric detection, the ratio of the two dynamic peaks is a direct parameter for analyte detection. The ratio of fluorescence peaks at I_{641} for HCA and at I_{539} for HCAP is employed as reporting value of ALP activity. Therefore, the larger the value of I_{641}/I_{539} reaches, the higher the sensitivity of the probe is. To optimize the concentration of HCAP used in the assay, HCAP with different concentrations was incubated in a constant ALP concentration (100 mU/mL) for 45 min, and the PL spectra were then recorded. As shown in Figure 3, the value of I_{641}/I_{539} increases with HCAP concentration from 1−20 μM. No significant change of the value of I_{641}/I_{539} is observed in the HCAP concentration ranging from 20−50 μM. However, when further increasing HCAP concentration up to 50 μM, the value of I_{641}/I_{539} decreases. Considering the fluorescence intensity of red channel from enzymatic product and larger value of I_{641}/I_{539}, we chose 40 μM HCAP as the probe concentration in the sensing experiments.

We then optimized the incubation time for the reaction-based catalytic process from HCAP to HCA. The PL spectra were measured every 2.5 min in the presence of 100 mU/mL of ALP and 40 μM HCAP. As shown in Figure 4, the HCAP in Tris-HCl buffer solution (pH = 9.2) emits yellow fluorescence before ALP addition. The fluorescence at 539 nm undergoes a gradual decrease upon increasing incubation time with a concomitant increase in the fluorescence intensity at 641 nm. An isoemissive point is observed at 603 nm. The fluorescence intensity at 641 nm reaches the maximum when the probe is incubated in the presence of ALP for 45 min, indicating that the enzymatic reaction reaches a saturated state.

2.5. ALP Activity Assay. To examine the possibility of quantitative analysis of ALP activity, we conducted experiments of concentration-dependent monitoring of enzymatic reaction. As shown in Figure 5A, the fluorescence intensity at 539 nm decreases, and that at 641 nm increases along with ALP activity ranging from 0 to 200 mU/mL. The corresponding peak intensities (I_{539} and I_{641}) are plotted in Figure 5B, and they vary as an exponential or logarithmic function with the activity of ALP. Interestingly, the ratiometric fluorescent plot (I_{641}/I_{539}) presents a linear relationship with ALP activity and high correlation coefficient (Figure 6). Meanwhile, the HCAP probe shows a good linearity in a broad range (0−150 mU/mL) with the limit of detection of 0.15 mU/mL. The outstanding

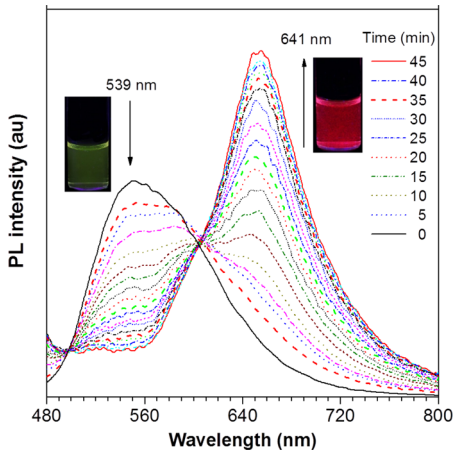

Figure 4. Time-dependent PL spectra of HCAP in Tris-HCl buffer solution (pH = 9.2) upon addition of ALP at 37 °C. (inset) Photographs taken under handheld UV lamp at 365 nm illumination of the corresponding solutions (left) before and (right) after incubation with ALP for 45 min. Concentration: HCAP (40 μM), ALP (100 mU/mL); excitation wavelength: 430 nm.

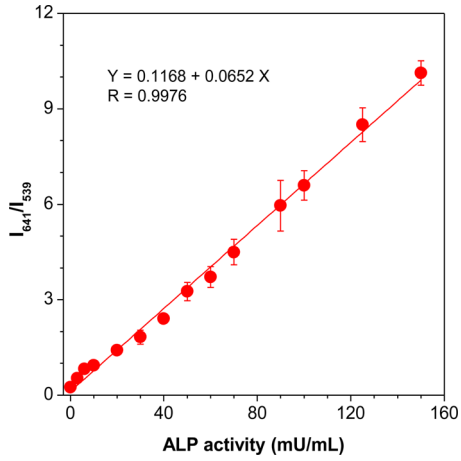

Figure 6. Ratiometric fluorescence response (I_{641}/I_{539}) of HCAP vs ALP concentration. Concentration of HCAP: 40 μM; excitation wavelength: 430 nm; incubation time: 45 min.

sensitivity should be attributed to the ratiometric fluorescent probe because it employs simultaneous readings of two fluorescent signal channels in the presence of an analyte, which minimizes some interfering factors with amplified signal output.[42,43]

As ALP is the most commonly assayed enzyme in practical blood examination, to explore its feasibility of ALP detection in real serum samples with HCAP, the experiment was conducted in buffer solution containing 1% fetal bovine serum (FBS). As shown in Supporting Information, Figure S15, although the fluorescence from the probe is strongly interfered by the serum, the red emission from HCA could still be observed, and the intensity after incubation with ALP increases by ~4.5-fold. In spite of the inferior performance in serum samples, the red fluorescence of HCA could be differentiated from strong background of the serum. In addition, the high-resolution mass spectrum confirmed the red fluorescent product was indeed HCA (Supporting Information, Figure S16). The particle size distribution was analyzed, and the corresponding fluorescence microscopic images were taken to further confirm the aggregation formation of HCA after incubation with ALP (Supporting Information, Figures S17 and S18).

2.6. Selectivity Test. Selectivity is another important parameter to evaluate the performance of bioprobes. To demonstrate that the HCAP probe is selective to ALP, a control experiment with other nonspecific enzymes including acetylcholinesterase (AChE), deoxyribonuclease (DNase), esterase, trypsin, and lysozyme was performed under the same conditions. As shown in Figure 7, a 9-fold fluorescence enhancement at 641 nm is observed only with the catalytic function of ALP. While other enzymes show negligible fluorescence changes in the red emission channel, the enzymes only have tiny interference on the ALP-catalyzed hydrolysis reaction. The result demonstrates that HCAP has excellent selectivity to ALP.

To further prove the red fluorescence enhancement is originated from the catalytic function of ALP rather than from other effects such as hydrophobic interaction and electrostatic interaction, we designed an inhibition experiment on ALP activity. It is known that the activity of ALP decreases much in the aqueous environment without Mg^{2+} and Zn^{2+} ions.[44] Since

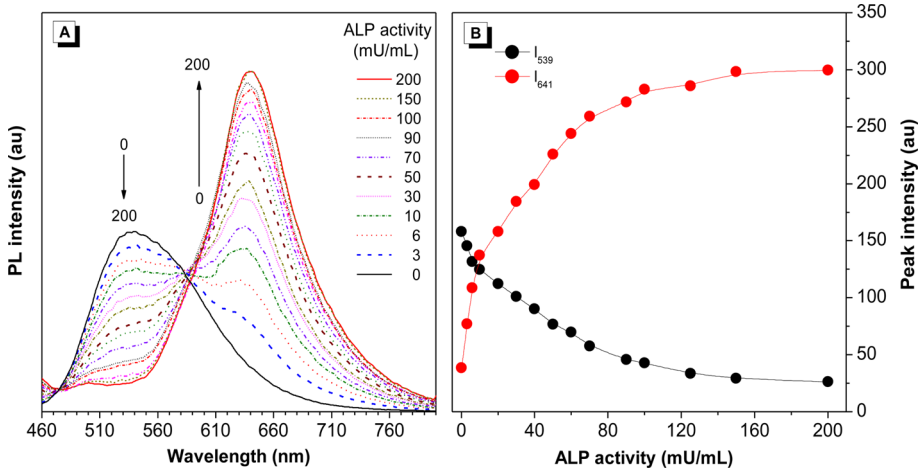

Figure 5. (A) PL spectra of HCAP in Tris-HCl buffer solution (pH = 9.2) in the presence of different concentrations of ALP at 37 °C. (B) Plot of peak intensities (red) at 641 nm and (black) at 539 nm vs ALP concentration; concentration of HCAP: 40 μM; excitation wavelength: 430 nm; incubation time: 45 min.

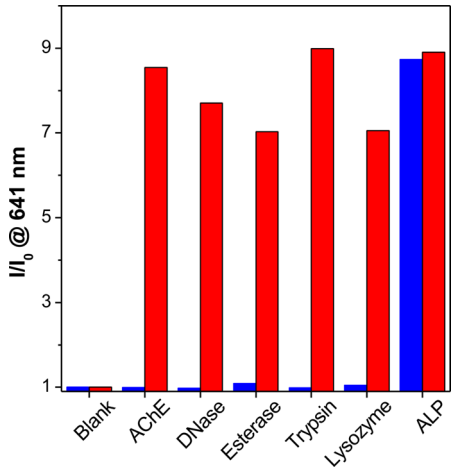

Figure 7. PL intensity change of HCAP (40 μM) at 641 nm upon incubation with different enzymes in Tris-HCl buffer (pH = 7.5, except for ALP pH = 9.2). Blue bars show the effect of different enzymes on the fluorescence intensity, and red bars show the presence of interfering enzymes on HCAP + ALP system.

ethylene diamine tetraacetic acid (EDTA) can chelate those metal ions in the active site of enzymes,[32,45,46] we hypothesize that HCAP will not be dephosphorylated by ALP and will retain yellow emission in the presence of EDTA. As shown in Figure 8, when the concentration of EDTA is below 1 mM, the

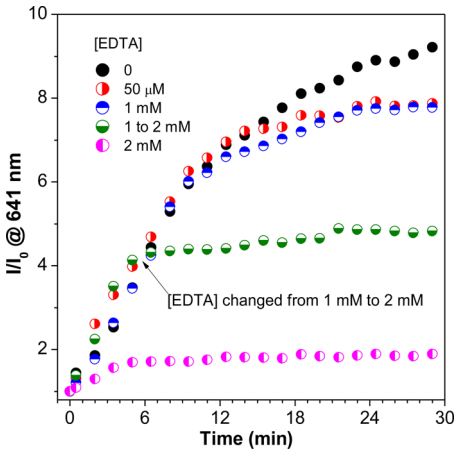

Figure 8. Plot of relative fluorescence intensity (I/I_0) of HCAP at 641 nm vs incubation time in the presence of different concentrations of EDTA (0, 50 μM, 1 mM, and 2 mM). Concentration: HCAP (40 μM), ALP (100 mU/mL); excitation wavelength: 430 nm.

fluorescence intensity of the probe is almost the same as the blank solution, suggesting there is no inhibition effect on ALP. As the Tris-HCl buffer solution contains 1 mM of Mg^{2+} and 50 μM of Zn^{2+}, EDTA will first chelate the metal ions in buffer solution. Thus, the activity of ALP remains. To verify our hypothesis, we first incubated HCAP with ALP in the presence of 1 mM EDTA for 5 min. Afterward, another 1 mM EDTA was further added to the solution, making the final concentration of EDTA equal to 2 mM. The enhancement of red emission of the probe immediately stops (olive dots), indicating that the ALP activity is inhibited. The fluorescence intensity remains at a low level when 2 mM EDTA is added at the beginning stage. This result clearly indicates that the red fluorescence enhancement is mainly due to the catalytic function of ALP but not to other interactions.

2.7. Imaging of Endogenic ALP in Living Cells. Inspired by the quantitative analysis of ALP in buffer solution and serum samples, we further investigated whether the probe was able to monitor endogenic ALP activity in living cells. We first examined cytotoxicity of HCAP by 3-(4,5-dimethyl-2-thiazolyl)-2,5-diphenyl-2*H*-tetrazolium bromide (MTT) assay. As shown in Figure 9, cell viability of HeLa cells remains at a high level even when the HCAP concentration is as high as 20 μM, suggesting that HCAP has good biocompatibility.

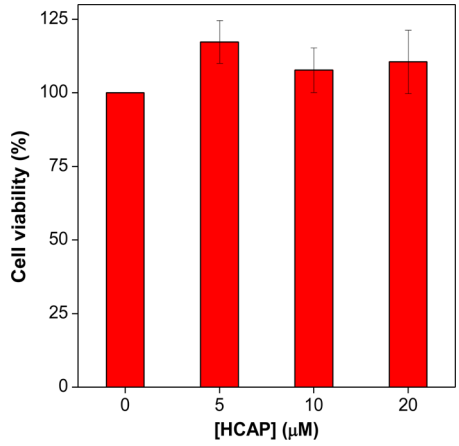

Figure 9. MTT assay of HCAP on HeLa cells.

As placental ALP could be expressed endogenically in HeLa cells, no exotic ALP is added in the experiments.[22,47] As shown in Figure 10D, the HeLa cells that incubated with 10 μM HCAP for 30 min displayed a clear orange fluorescence in the cell cytoplasm. However, there is no fluorescence observed from the cells untreated with HCAP (Figure 10B) as well as those preincubated with the ALP inhibitor, levamisole (Figure 10F). Meanwhile, it is found that the emission color of HCA is slightly blue-shifted when compared to the emission in buffer solution. To verify that the orange fluorescence is indeed originated from HCA, we used synthetic HCA to stain HeLa cells under the same conditions. The result reveals that the orange fluorescence from the HCAP probe incubated with ALP is the same as that from synthetic HCA (Supporting Information, Figure S19). The possible reason for the blue-shifted emission is that HCA adopted a more twisted configuration in cells due to the interaction with biomacromolecules and thus results in less conjugation of HCA and a more hydrophobic microenvironment for the product. The experimental result suggests that HCAP is converted to HCA efficiently with the catalysis of endogenic ALP from HeLa cells. Thus, HCAP can potentially act as a light-up probe for ALP detection in situ.

To further investigate the behavior of HCAP inside and outside of cells, confocal laser scanning microscopy was employed. By taking advantage of the two distinct emissions of HCA and HCAP, we can verify whether the probe is hydrolyzed inside or outside of cells. If HCAP is able to enter the cells and is hydrolyzed to HCA inside the cell, the emission from ALP-inhibited cells in green channel should give brighter image than the cells without inhibitor. As shown in Figure 11, the HeLa cells show orange fluorescence after incubation with HCAP (Figure 11C). Similarly, the orange fluorescence in the

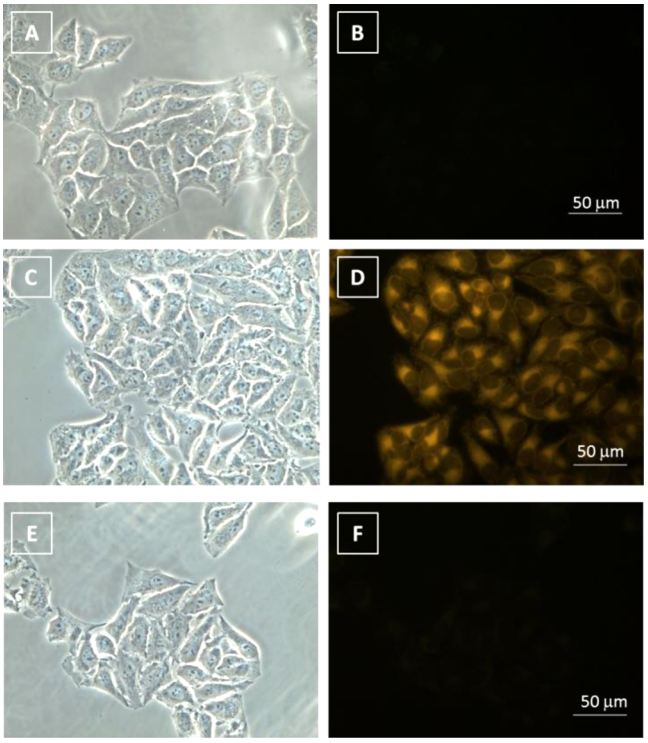

Figure 10. Fluorescence images of HeLa cells in the absence or presence of HCAP. (A, C, E) Bright field images corresponding to the fluorescence images with (B) no HCAP, (D) HCAP (10 μM), and (F) HCAP (10 μM) and levamisole (5 mM). Excitation wavelength: 460 nm ~490 nm.

HeLa cells is weaker when the cells are pretreated with levamisole (Figure 11F).[48] Unexpectedly, when comparing the emission in the green channel, the fluorescence observed in ALP-inhibited cells is even weaker than that in noninhibited cells (Figure 11B,E), which indicates that HCAP is not able to enter the cells and that the weak emission in the green channel should be ascribed to short-wavelength part of the emission peak from HCA. Thus, it can be concluded that the HCAP is hydrolyzed by the ALP secreted by cells, and the resulting HCA formed in intercellular fluids could enter the cells and show orange fluorescence.

3. CONCLUSIONS

Through a simple modification of 2′-hydroxychalcone, we have developed a novel ratiometric fluorescent bioprobe with AIE characteristics and ESPIT property for ALP activity assay in buffers and serum samples. In the presence of ALP, the emission of the bioprobe is changed from greenish-yellow to red. The bioprobe enables ALP assay in the concentration range of 0−150 mU/mL with a detection limit of 0.15 mU/mL, which is outstanding compared with previous literature. Moreover, the red emission of the enzymatic residue prevents the autofluorescence interference from serum sample. The fluorescent probe could also be applied for detection of ALP in intercellular fluids and visualization of the corresponding living cells. The molecular design strategy provides a comprehensive example for utilizing natural products to construct ratiometric fluorescent probes with high sensitivity and red fluorescence emission in aggregated state.

4. EXPERIMENTAL SECTION

4.1. Materials and Instrumentation. All chemicals and reagents were commercially available and used as received. THF and DCM were distilled from sodium benzophenone ketyl and calcium hydride, respectively, under nitrogen immediately prior to use. 2′-hydroxyacetophenone, 4-dimethylamino benzaldehyde, sodium hydride, diethyl chlorophosphate, iodotrimethylsilane, and alkaline phosphatase (ALP) from bovine intestinal mucosa were purchased from Aldrich. Levamisole was purchased from TCI. Fetal bovine serum (FBS) and 3-(4,5-dimethylthiazol-2-yl)-2,5-diphenyltetrazolium bromide (MTT)

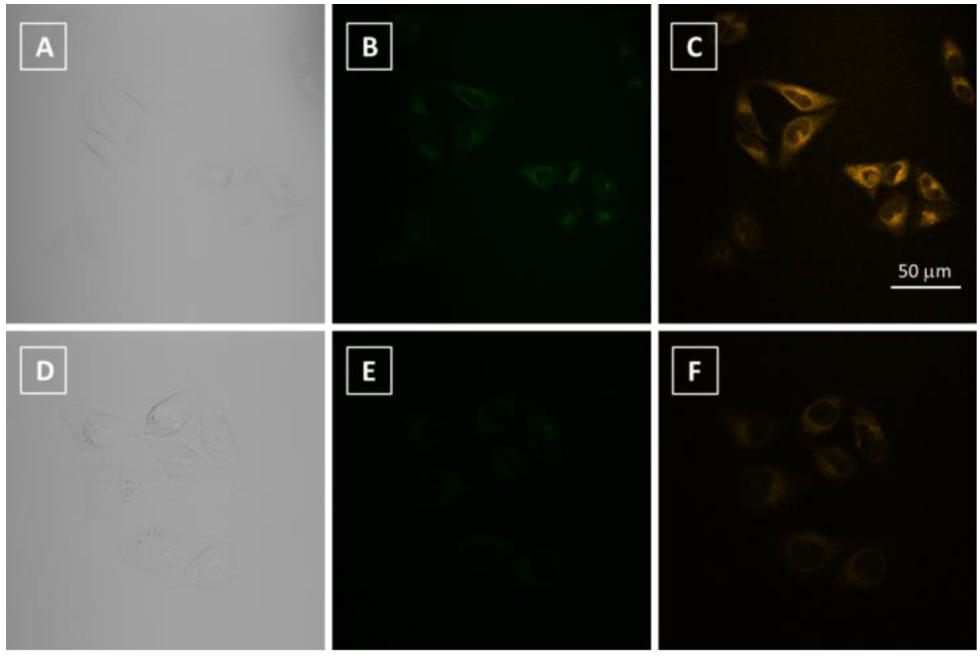

Figure 11. Confocal lasing scanning microscopic (CLSM) images of HeLa cells (A−C) incubated with HCAP and (D−F) HCAP with inhibitor capturing with different emission channels. Concentration: HCAP (10 μM), levamisole (5 mM) (B, E) channel 1: 433−516 nm; (C, F) channel 2: 545−607 nm.

were purchased from Invitrogen. Tris-HCl buffer (pH = 9.2, 10 mM) was prepared with pure water from a Millipore filtration system. Other enzymes used in the selectivity test were purchased from Aldrich. ^{1}H, ^{13}C, and ^{31}P NMR spectra were measured on a Bruker ARX 400 NMR spectrometer using $CDCl_3$ and CD_3OD as solvents, and tetramethylsilane (TMS; δ = 0 ppm) was chosen as internal reference. UV spectra were measured on a Biochrom Libra S80PC double beam spectrometer. Photoluminescence (PL) spectra were recorded on a PerkinElmer LS 55 spectrofluorometer. High-resolution mass spectra (HRMS) were recorded on a GCT Premier CAB 048 mass spectrometer operating in MALDI-TOF mode. Particle sizes were determined using a Brookhaven ZetaPlus potential analyzer (Brookhaven instruments corporation, USA). Fluorescent images were taken on a fluorescent microscope (BX41 Microscope), and confocal lasing scanning microscopic (CLSM) images were obtained on a confocal microscope (Zeiss Laser Scanning Confocal Microscope; LSM7 DUO) using ZEN 2009 software (Carl Zeiss).

4.2. Synthesis. *4-Dimethylamino-2′-hydroxychalcone (HCA).* To a solution of 4-dimethylbenzaldehyde (12 mmol, 1.79 g) and 2′-hydroxyacetophenone (13.2 mmol, 1.80 g) in EtOH (30 mL), KOH (50 mmol, 2.8 g) in water was added and stirred at room temperature for 24 h. The reaction mixture was neutralized with dilute HCl until the pH value was adjusted to 7.0. The precipitates were collected through suction filtration and washed with ethanol three times. The obtained residue was further purified by silica gel chromatography with hexane/ethyl acetate (5:1) as eluent to afford the desired product (700 mg, 2.62 mmol) as deep red crystals. Yield = 22%. ^{1}H NMR (400 MHz, $CDCl_3$): δ (TMS, ppm) 13.23 (s, 1H), 7.93−7.90 (m, 2H), 7.58−7.56 (m, 2H), 7.47−7.43 (m, 2H), 7.02−7.00 (m, 1H), 6.92 (t, 1H), 6.70−6.68 (d, 2H), 3.05 (s, 6H). ^{13}C NMR (100 MHz, $CDCl_3$): δ (TMS, ppm) 192.9, 162.8, 151.7, 145.9, 135.0, 130.2, 128.7, 121.7, 119.8, 117.8, 113.6, 111.2, 39.5. HRMS (MALDI-TOF), m/z calcd. for $C_{17}H_{17}NO_2$: 267.1259; found 267.1258 (M^+).

2-(3-(4-(Dimethylamino)phenyl)acryloyl)phenyl Diethyl Phosphate (HCAPE). To a solution of HCA (1 mmol, 267 mg) and NaH (2 mmol, 80 mg) in distilled THF (20 mL), diethyl chlorophosphate (0.3 mL, 2.0 mmol) was added dropwise under nitrogen. The reaction mixture was stirred at room temperature for 2 h. The resulting solution was quenched with water (2 mL), and the solvent was evaporated under reduced pressure. The crude mixture was extracted with DCM three times. The combined organic layer was dried over $MgSO_4$ and filtered, and the solvent was evaporated under reduced pressure. The crude product was purified by silica gel chromatography with hexane/ethyl acetate (2:1) as eluent to afford the desired product (370 mg, 0.92 mmol) as orange gel-like solid. Yield = 92%. ^{1}H NMR (400 MHz, $CDCl_3$): δ (TMS, ppm) 7.55−7.46 (m, 6H), 7.25−7.22 (d, 1H), 7.06−7.02 (d, 1H), 6.67−6.65 (d, 2H), 4.15−4.12 (m, 4H), 3.03 (s, 6H), 1.24−1.23 (t, 6H). ^{13}C NMR (100 MHz, $CDCl_3$): δ (TMS, ppm) 191.6, 151.5, 147.4, 145.8, 132.0, 132.0, 131.2, 129.9, 129.4, 124.3, 121.6, 120.8, 119.8, 119.8, 111.1, 64.3, 64.2, 39.5, 15.4, 15.3. ^{31}P NMR (162 MHz, $CDCl_3$): δ (TMS, ppm) −7.26. HRMS (MALDI-TOF), m/z calcd. for $C_{21}H_{26}NO_5P$: 403.1549; found 403.1549 (M^+).

2-(3-(4-(Dimethylamino)phenyl)acryloyl)phenyl Phosphate (HCAP). To a solution of HCAPE (201 mg, 0.5 mmol) in dry DCM (25 mL) was added iodotrimethylsilane (0.28 mL, 2.0 mmol) dropwise under nitrogen at 0 °C. The reaction mixture was stirred for 3 h at room temperature before the addition of MeOH (2 mL). After the mixture was stirred for another 0.5 h, the solvent was removed under reduced pressure. The crude product was purified by silica gel chromatography with DCM/methanol (10:1) as eluent to afford HCAP (73 mg, 0.21 mmol) as orange gel-like solid. Yield = 42%. ^{1}H NMR (400 MHz, CD_3OD): δ (TMS, ppm) 7.77−7.74 (d, 2H), 7.62−7.52 (m, 4H), 7.44−7.38 (m, 2H), 7.28 (t, 2H), 3.02 (s, 6H). ^{13}C NMR (100 MHz, CD_3OD): δ (TMS, ppm) 191.9, 149.1, 145.8, 142.8, 131.9, 131.6, 131.2, 129.8, 129.1, 125.2, 123.7, 120.3, 117.4, 43.0. ^{31}P NMR (162 MHz, CD_3OD): δ (TMS, ppm) −6.13. HRMS (MALDI-TOF), m/z calcd. for $C_{17}H_{18}NO_5P$: 347.0923; found: 347.0916 (M^+).

4.3. Preparation of Aggregates. Stock THF solution of HCA with a concentration of 2 mM was prepared. An aliquot (0.1 mL) of the stock solution was transferred to a 10 mL volumetric flask. After adding an appropriate amount of THF, water was added dropwise under vigorous stirring to furnish 20 μM THF/water mixtures with water fractions (f_w) of 0−99 vol %. Measurement of PL, particle size analyses, and fluorescent microscopy of the resulting mixtures were carried out.

4.4. Optimization of HCAP Concentration and Incubation Time for ALP Activity Assay. Solutions of HCAP (1−100 μM) were prepared by mixing Tris-HCl buffer (10 mM, pH = 9.2) and a certain amount of HCAP stock solution (2 mM), rendering the final concentration of HCAP ranging from 1 μM to 100 μM. Each testing sample was added in 100 mU/mL of ALP and then incubated for 45 min at 37 °C. Afterward, the PL spectra of resulting solutions were recorded at the same conditions. For the optimization of ALP, 100 mU/mL of ALP was added into the buffer solution of HCAP (40 μM), immediately followed by PL scanning. The enzymatic hydrolysis process was monitored by the PL spectral measurements, which scanned at intervals of 90 s.

4.5. ALP Activity Assay. Different amounts of ALP stock solutions (20 U/mL) were added into the probe solution of HCAP (2 mL, 40 μM) to yield final concentrations of ALP from 0 to 200 mU/mL. PL measurements were carried out after the prepared solutions were incubated at 37 °C for 45 min. For the selectivity test, all the interfering enzymes were tested under the same conditions with ALP.

4.6. Cell Culture. HeLa cells were cultured in the minimum Eagle's essential medium containing 10% FBS and antibiotics (100 units/mL penicillin and 100 μg/mL streptomycin) in a 5% CO_2 and 90% humidity incubator at 37 °C.

4.7. Cell Imaging. HeLa cells were grown overnight on a 35 mm Petri dish with a coverslip or a plasma-treated 25 mm round coverslip mounted to the bottom of a 35 mm Petri dish with an observation window. The living cells were stained with 10 mM HCA for 30 min, 20 mM HCAP for 30 min, or preincubated with inhibitor, levamisole (5 mM) for 10 min followed by incubation with 20 mM HCAP for 20 min. The cells were imaged under a fluorescent microscope (BX41 Microscope) using excitation filter = 460−490 nm and dichroic mirror = 505 nm. The preparation process of cell samples in CLSM imaging was the same as that in fluorescence microscopic imaging. HCAP was excited at 405 nm (6% laser power), and the fluorescence was collected at channel 1 (433−516 nm) and channel 2 (545−607 nm), respectively.

4.8. Cell Viability Evaluated by MTT Assay. Viability of the cells was assayed using cell proliferation Kit I with the absorbance of 595 nm being detected using a PerkinElmer Victor plate reader. Eight thousand cells were seeded per well in a 96-well plate. After overnight culture, various concentrations of HCAP were added into the 96-well plate. After 8 h of treatment, 10 μL of 3-(4,5-dimethyl-2-thiazolyl)-2,5-diphenyltetrazolium bromide (MTT) solution (5 mg/mL in phosphate buffer solution) was added into the each well. After 4 h of incubation at 37 °C, 100 μL of solubilization solution containing 10% sodium dodecyl sulfate and 0.01 M HCl was added to dissolve the purple crystals. After 4 h of incubation, the optical density readings at 595 nm were taken using a plate reader. Each of the experiments was performed at least three times.

■ ASSOCIATED CONTENT

Ⓢ Supporting Information

Characterization data of HCA, HCAPE, and HCAP; absorption spectra of HCA and HCAP and emission spectrum of HCA in solid state; pH-dependent emission spectra of HCA; particle size distribution of HCAP after incubation with ALP; fluorescence microscopic images of HCA tiny crystals in the buffer of HCAP incubated with ALP; time-dependent emission spectra of HCAP in buffer solution with FBS upon addition of ALP; fluorescence images of HeLa cells stained by HCA. This material is available free of charge via the Internet at http://pubs.acs.org.

AUTHOR INFORMATION

Corresponding Authors

*Email: tangbenz@ust.hk. (B.Z.T.)
*E-mail: cheliub@nus.edu.sg. (B.L.)

Author Contributions

‖Z.S. and R.T.K.K. contributed equally to this work.

Notes

The authors declare no competing financial interest.

ACKNOWLEDGMENTS

This work was partially supported by the National Basic Research Program of China (973 Program; 2013CB834701), the Research Grants Council of Hong Kong (604711, 604913, HKUST2/CRF/10, and N_HKUST620/11), Innovation and Technology Commission (ITCPD/17-9), the University Grants Committee of Hong Kong (AoE/P-03/08), and the Singapore Ministry of Defense (R279-000-340-232). B.Z.T. is grateful for the support from the Guangdong Innovative Research Team Program of China (201101C0105067115).

REFERENCES

(1) Arya, S. K.; Bhansali, S. Lung Cancer and Its Early Detection Using Biomarker-Based Biosensors. *Chem. Rev.* **2011**, *111*, 6783.

(2) Medley, C. D.; Bamrungsap, S.; Tan, W.; Smith, J. E. Aptamer-Conjugated Nanoparticles for Cancer Cell Detection. *Anal. Chem.* **2011**, *83*, 727.

(3) Feng, X.; Feng, F.; Yu, M.; He, F.; Xu, Q.; Tang, H.; Wang, S.; Li, Y.; Zhu, D. Synthesis of a New Water-Soluble Oligo-(phenylenevinylene) Containing a Tyrosine Moiety for Tyrosinase Activity Detection. *Org. Lett.* **2008**, *10*, 5369.

(4) Li, Z.; Li, X.; Gao, X.; Zhang, Y.; Shi, W. Nitroreductase Detection and Hypoxic Tumor Cell Imaging by a Designed Sensitive and Selective Fluorescent Probe, 7-[(5-Nitrofuran-2-yl)methoxy]-3H-phenoxazin-3-one. *Anal. Chem.* **2013**, *85*, 3926.

(5) Li, L.; Zhang, C. W.; Chen, G. Y. J.; Zhu, B.; Chai, C.; Xu, Q. H.; Tan, E. K.; Zhu, Q.; Lim, K. L.; Yao, S. Q. A Sensitive Two-Photon Probe to Selectively Detect Monoamine Oxidase B Activity in Parkinson's Disease Models. *Nat. Commun.* **2014**, *5*, 3276.

(6) Wang, L.; Pu, K.-Y.; Li, J.; Qi, X.; Li, H.; Zhang, H.; Fan, C.; Liu, B. A Graphene-Conjugated Oligomer Hybrid Probe for Light-Up Sensing of Lectin and *Escherichia Coli*. *Adv. Mater.* **2011**, *23*, 4386.

(7) Syakalima, M.; Takiguchi, M.; Yasuda, J.; Hashimoto, A. A Study of Liver and Corticosteroid-Induced Alkaline Phosphatase Isoenzymes Activities associated with Glucocorticoid Hepatopathy in the Dog. *Jpn. J. Vet. Res.* **1998**, *46*, 3.

(8) Coleman, J. E. Structure and Mechanism of Alkaline Phosphatase. *Annu. Rev. Biophys. Biomol. Struct.* **1992**, *21*, 441.

(9) Ooi, K.; Shiraki, K.; Morishita, Y.; Nobori, T. High-Molecular Intestinal Alkaline Phosphatase in Chronic Liver Diseases. *J. Clin. Lab. Anal.* **2007**, *21*, 133.

(10) Wolf, P. L. Clinical Significance of Serum High-Molecular-Mass Alkaline Phosphatase, Alkaline Phosphatase−Lipoprotein-X Complex, and Intestinal Variant Alkaline Phosphatase. *J. Clin. Lab. Anal.* **1994**, *8*, 172.

(11) Gyurcsanyi, R. E.; Bereczki, A.; Nagy, G.; Neuman, M. R.; Lindner, E. Amperometric Microcells for Alkaline Phosphatase Assay. *Analyst* **2002**, *127*, 235.

(12) Chung, I. S.; Taticek, R. A.; Shuler, M. L. Production of Human Alkaline Phosphatase, a Secreted, Glycosylated Protein, from a **B**aculovirus Expression System and the Attachment-Dependent Cell Line *Trichoplusia ni* BTI-Tn 5B1−4 Using a Split-Flow, Air-Lift Bioreactor. *Biotechnol. Prog.* **1993**, *9*, 675.

(13) Arai, T.; Nishijo, T.; Matsumae, Y.; Zhou, Y.; Ino, K.; Shiku, H.; Matsue, T. Noninvasive Measurement of Alkaline Phosphatase Activity in Embryoid Bodies and Coculture Spheroids with Scanning Electrochemical Microscopy. *Anal. Chem.* **2013**, *85*, 9647.

(14) Shi, H. B.; Kwok, R. T. K.; Liu, J. Z.; Xing, B. G.; Tang, B. Z.; Liu, B. Real-Time Monitoring of Cell Apoptosis and Drug Screening Using Fluorescent Light-Up probe with Aggregation-Induced Emission Characteristics. *J. Am. Chem. Soc.* **2012**, *134*, 17972.

(15) Shi, H. B.; Liu, J. Z.; Geng, J. L.; Tang, B. Z.; Liu, B. Specific Detection of Integrin $\alpha_v\beta_3$ by Light-Up Bioprobe with Aggregation-Induced Emission Characteristics. *J. Am. Chem. Soc.* **2012**, *134*, 9569.

(16) Zhang, H.; Fan, J.; Wang, J.; Dou, B.; Zhou, F.; Gao, J.; Cao, Z.; Zhao, W.; Peng, X. Fluorescence Discrimination of Cancer from Inflammation by Molecular Response to COX-2 Enzymes. *J. Am. Chem. Soc.* **2013**, *135*, 17469.

(17) Karton-Lifshin, N.; Segal, E.; Omer, L.; Portnoy, M.; Satchi-Fainaro, R.; Shabat, D. A Unique Paradigm for a Turn-ON Near-Infrared Cyanine-Based Probe: Noninvasive Intravital Optical Imaging of Hydrogen Peroxide. *J. Am. Chem. Soc.* **2011**, *133*, 10960.

(18) Guo, T.; Cui, L.; Shen, J.; Zhu, W.; Xu, Y.; Qian, X. A Highly Sensitive Long-Wavelength Fluorescence Probe for Nitroreductase and Hypoxia: Selective Detection and Quantification. *Chem. Commun.* **2013**, *49*, 10820.

(19) Jia, L.; Xu, J. P.; Li, D.; Pang, S. P.; Fang, Y.; Song, Z. G.; Ji, J. Fluorescence Detection of Alkaline Phosphatase Activity with β-Cyclodextrin-Modified Quantum Dots. *Chem. Commun.* **2010**, *46*, 7166.

(20) Zhang, L.; Zhao, J.; Duan, M.; Zhang, H.; Jiang, J.; Yu, R. Inhibition of dsDNA-Templated Copper Nanoparticles by Pyrophosphate as a Label-Free Fluorescent Strategy for Alkaline Phosphatase Assay. *Anal. Chem.* **2013**, *85*, 3797.

(21) Chen, Q.; Bian, N.; Cao, C.; Qiu, X. L.; Qi, A. D.; Han, B. H. Glucosamine Hydrochloride Functionalized Tetraphenylethylene: A Novel Fluorescent Probe for Alkaline Phosphatase Based on the Aggregation-Induced Emission. *Chem. Commun.* **2010**, *46*, 4067.

(22) Kim, T. I.; Kim, H.; Choi, Y.; Kim, Y. A Fluorescent Turn-On Probe for the Detection of Alkaline Phosphatase Activity in Living Cells. *Chem. Commun.* **2011**, *47*, 9825.

(23) Jiao, H.; Chen, J.; Li, W.; Wang, F.; Zhou, H.; Li, Y.; Yu, C. Nucleic Acid-Regulated Perylene Probe-Induced Gold Nanoparticle Aggregation: A New Strategy for Colorimetric Sensing of Alkaline Phosphatase Activity and Inhibitor Screening. *ACS Appl. Mater. Interfaces* **2014**, *6*, 1979.

(24) Hong, Y.; Lam, J. W. Y.; Tang, B. Z. Aggregation-Induced Emission: Phenomenon, Mechanism and Applications. *Chem. Commun.* **2009**, 4332.

(25) Hong, Y.; Lam, J. W. Y.; Tang, B. Z. Aggregation-Induced Emission. *Chem. Soc. Rev.* **2011**, *40*, 5361.

(26) Chen, S.; Hong, Y.; Liu, Y.; Liu, J.; Leung, C. W. T.; Li, M.; Kwok, R. T. K.; Zhao, E.; Lam, J. W. Y.; Yu, Y.; Tang, B. Z. Full-Range Intracellular pH Sensing by an Aggregation-Induced Emission-Active Two-Channel Ratiometric Fluorogen. *J. Am. Chem. Soc.* **2013**, *135*, 4926.

(27) Ding, D.; Li, K.; Liu, B.; Tang, B. Z. Bioprobes Based on AIE Fluorogens. *Acc. Chem. Res.* **2013**, *46*, 2441.

(28) Wang, M.; Zhang, G.; Zhang, D.; Zhu, D.; Tang, B. Z. Fluorescent Bio/Chemosensors Based on Silole and Tetraphenylethene Luminogens with Aggregation-Induced Emission Feature. *J. Mater. Chem.* **2010**, *20*, 1858.

(29) Liu, Y.; Deng, C.; Tang, L.; Qin, A.; Hu, R.; Sun, J. Z.; Tang, B. Z. Specific Detection of $_D$-Glucose by a Tetraphenylethene-Based Fluorescent Sensor. *J. Am. Chem. Soc.* **2011**, *133*, 660.

(30) Yu, Y.; Qin, A.; Feng, C.; Lu, P.; Ng, K. M.; Luo, K. Q.; Tang, B. Z. An Amine-Reactive Tetraphenylethylene Derivative for Protein Detection in SDS-PAGE. *Analyst* **2012**, *137*, 5592.

(31) Gu, X.; Zhang, G.; Wang, Z.; Liu, W.; Xiao, L.; Zhang, D. A New Fluorometric Turn-On Assay for Alkaline Phosphatase and Inhibitor Screening Based on Aggregation and Deaggregation of Tetraphenylethylene Molecules. *Analyst* **2013**, *138*, 2427.

(32) Liang, J.; Kwok, R. T. K.; Shi, H.; Tang, B. Z.; Liu, B. Fluorescent Light-Up Probe with Aggregation-Induced Emission Characteristics for Alkaline Phosphatase Sensing and Activity Study. *ACS Appl. Mater. Interfaces* **2013**, *5*, 8784.

(33) Zhao, J.; Ji, S.; Chen, Y.; Guo, H.; Yang, P. Excited State Intramolecular Proton Transfer (ESIPT): from Principal Photophysics to the Development of New Chromophores and Applications in Fluorescent Molecular Probes and Luminescent Materials. *Phys. Chem. Chem. Phys.* **2012**, *14*, 8803.
(34) Goswami, S.; Das, S.; Aich, K.; Pakhira, B.; Panja, S.; Mukherjee, S. K.; Sarkar, S. A Chemodosimeter for the Ratiometric Detection of Hydrazine Based on Return of ESIPT and Its Application in Live-Cell Imaging. *Org. Lett.* **2013**, *15*, 5412.
(35) Li, G.; Zhu, D.; Liu, Q.; Xue, L.; Jiang, H. Rapid Detection of Hydrogen Peroxide Based on Aggregation Induced Ratiometric Fluorescence Change. *Org. Lett.* **2013**, *15*, 924.
(36) Murale, D. P.; Kim, H.; Choi, W. S.; Churchill, D. G. Highly Selective Excited State Intramolecular Proton Transfer (ESIPT)-Based Superoxide Probing. *Org. Lett.* **2013**, *15*, 3946.
(37) Kim, T.; Kang, H. J.; Han, G.; Chung, S. J.; Kim, Y. A Highly Selective Fluorescent ESIPT Probe for the Dual Specificity Phosphatase MKP-6. *Chem. Commun.* **2009**, *2*, 5895.
(38) Teshima, T.; Takeishi, M.; Arai, T. Red Fluorescence from Tautomers of 2′-Hydroxychalcones Induced by Intramolecular Hydrogen Atom Transfer. *New J. Chem.* **2009**, *33*, 1393.
(39) Liu, Z.; Fang, Q.; Yu, W.; Xue, G.; Cao, D.; Jiang, M. 2′-Hydroxy-4″-Dimethylamino-Chalcone. *Acta Crystallogr., Sect. C: Cryst. Struct. Commun.* **2002**, *58*, o445−o446.
(40) Norikane, Y.; Itoh, H.; Arai, T. Photochemistry of 2′-Hydroxychalcone. One-Way Cis−Trans Photoisomerization Induced by Adiabatic Intramolecular Hydrogen Atom Transfer. *J. Phys. Chem. A* **2002**, *106*, 2766.
(41) Iqbal, J. An Enzyme Immobilized Micro-Assay in Capillary Electrophoresis for Characterization and Inhibition Studies of Alkaline Phosphatases. *Anal. Biochem.* **2011**, *414*, 226−231.
(42) Luxami, V.; Verma, M.; Rani, R.; Paul, K.; Kumar, S. FRET-Based Ratiometric Detection of Hg2+ and Biothiols Using Naphthalimide-Rhodamine Dyads. *Org. Biomol. Chem.* **2012**, *10*, 8076.
(43) Lee, S. W.; Rhee, H. W.; Chang, Y. T.; Hong, J. I. Ratiometric Fluorescent Probes for Hydrogen Peroxide from a Focused Library. *Chem.—Eur. J.* **2013**, *19*, 14791.
(44) Bosron, W. F.; Kennedy, F. S.; Vallee, B. L. Zinc and Magnesium Content of Alkaline Phosphatase from *Escherichia Coli*. *Biochemistry* **1975**, *14*, 2275.
(45) Adak, S.; Bhattacharyya, D. K.; Mazumder, A.; Bandyopadhyay, U.; Banerjee, R. K. Concurrent Reduction of Iodine and Oxidation of EDTA at the Active Site of Horseradish Peroxidase: Probing the Iodine Binding Site by Optical Difference Spectroscopy and Steady State Kinetic Analysis for the Formation of Active Enzyme-I^+-EDTA Ternary Complex for Iodine Reductase Activity. *Biochemistry* **1995**, *34*, 12998.
(46) Belle, H. V. Kinetics and Inhibition of Alkaline Phosphatases from Canine Tissues. *Biochim. Biophys. Acta* **1972**, *289*, 158.
(47) Herz, F.; Schermer, A.; Halwer, M.; Bogart, L. H. Alkaline Phosphatase in HT-29, a Human Colon Cancer Cell Line: Influence of Sodium Butyrate and Hyperosmolality. *Arch. Biochem. Biophys.* **1981**, *210*, 581.
(48) Sanecki, R. K.; Hoffmann, W. E.; Gelberg, H. B.; Dorner, J. L. Subcellular Location of Corticosteroid-Induced Alkaline Phosphatase in Canine Hepatocytes. *Vet. Pathol.* **1987**, *24*, 296.